Asian Journal of Chemistry; Vol. 26, No. 21 (2014), 7102-7104

ASIAN JOURNAL OF CHEMISTRY

http://dx.doi.org/10.14233/ajchem.2014.16501

Akaganeite/Silica Yolk-Shell Structures for Removal of Cr(VI)

WEIWEI WANG* and JIALIANG YAO

School of Materials Science and Engineering, Shandong University of Technology, 12 Zhang Zhou Road, Zibo 255091, Shandong, P.R. China

*Corresponding author: Fax: +86 533 2781660; Tel: +86 533 2782198; E-mail: weiweiwangsd@aliyun.com

Received: 9 October 2013; *Accepted*: 12 March 2014; *Published online*: 30 September 2014; AJC-16079

Akaganeite (β-FeOOH) with a tunnel structure represents inexpensive and abundant materials for removal of heavy metal ions. To improve its adsorption property, silica layer was coated on the surface of β-FeOOH, which was dissolved by reacting with $NaBH_4$ and re-grew to form silica porous layer and interior voids. β-FeOOH/silica yolk-shell structures were obtained. The effects of silica layer thicknesses and reaction time on the formation of yolk-shell structures were investigated. β-FeOOH/silica yolk-shell structures were used as adsorbent for removal of heavy metal ions present in water and showed a strong Cr(VI) ions removal capacity. The existence of a large number of pores and interior voids in yolk-shell structures was important for the improvement of adsorption ability.

Keywords: Porous materials, Akaganeite, Yolk-shell structures.

INTRODUCTION

Hollow particles with functional cores inside, known as yolk-shell structures or rattle structures, have attracted considerable attention in the past decades[1-3]. With the combination of the functionalities of cores and shells and unique structures, novel properties could be introduced to the yolk-shell structures. The incorporation of movable Fe_3O_4 as cores into SnO_2 hollow shells exhibit significantly enhanced microwave absorption properties[2]. FePt@CoS_2 yolk-shell nanocrystals could be used as a potent agent to kill HeLa cells[4]. Mesoporous titania yolk-shell structures and magnetic TiO_2 rattle-type nanoparticles showed enhanced photocatalytic activity due to multiple reflections of UV light within the interior voids[5,6].

Coating of nanoparticles can significantly improve their stability and biocompatibility. Silica was recognized as a good candidate for a coating material because it is chemical stable and relatively biocompatible. In particular, porous silica material is an excellent candidate due to its stability in aqueous solution and easy access for ions to the core, which significantly improves the heavy metal ions adsorption property. It has been reported that silica nanospheres could be converted into surface-rough SiO_2 nanoparticles or silica hollow sphere by reaction with $NaBH_4$[7-9]. In this study, we report on a novel design of β-FeOOH/silica yolk-shell structures that have a β-FeOOH core and porous silica layer. The abundant holes and ions accessibility through the pores allow for an efficient adsorption property. This was demonstrated in the adsorption behaviors of Cr(VI) on β-FeOOH/silica yolk-shell structures.

EXPERIMENTAL

Ferric chloride ($FeCl_3\cdot 6H_2O$), polyvinylpyrrolidone (PVP), sodium borohydride ($NaBH_4$), tetraethylorthosilicate (TEOS), ammonia ($NH_3\cdot H_2O$), ethanol (C_2H_5OH) and potassium dichromate ($K_2Cr_2O_7$) were purchased from Sinopharm Chemical Reagent Co. Ltd. and used as received without further purification.

General procedure: β-FeOOH/SiO_2 core/shell structures: β-FeOOH (4.8 mM, prepared by the reported method[9] and aqueous NH_3 were added to the mixture solution of ethanol and distilled water (the volume ratio between ethanol and distilled water was 4:1). After ultrasonic treatment for 15 min, TEOS was added to the above solution. The resulting suspension was stirred at room temperature for 10 h. The product was separated by centrifugation and washed with absolute ethanol. β-FeOOH/SiO_2 with different thicknesses of SiO_2 were obtained by changing the mole ratio of ammonia to TEOS and coating steps. The mole ratio of ammonia to TEOS was 10:1 for sample 1 and 2:1 for sample 2. A second coating step was performed for sample 3 by using sample 1 (4.8 mM) as the precursor. The mole ratio of ammonia to TEOS was 2:1.

β-FeOOH/SiO_2 yolk-shell structures: β-FeOOH/SiO_2 core-shell structures (29 g/L) and PVP (5 mM) were dispersed in distilled water. After ultrasonic treatment for 15 min, $NaBH_4$ (1.5 M) was added to the above suspension. The suspension was heated at 50 °C for different times. The following process was the same as that of sample 1.

Cr(VI) adsorption experiments: Potassium dichromate was vacuum-dried at 120 °C for 2 h. Then $K_2Cr_2O_7$ was dissolved in deionized water to form stock solution. Samples (0.4 g/L) were added to 25 mL of Cr(VI) stock solutions with different initial concentrations (5, 15, 25, 50, 100, 200 and 400 mg/L). These solutions were stirred at room temperature for 48 h. The amount of Cr(VI) adsorbed at equilibrium (q_e, mg/g) was calculated from formula: $q_e = (C_0-C_e)V/m$, where C_0 and C_e represent the concentration of Cr(VI) before and after removal process, respectively. V is the solution volume and m is the weight of the adsorbent.

Detection method: X-ray powder diffraction (XRD) patterns were recorded using a D8 ADVANCE X-ray diffractometer (λ = 1.5406 Å). Transmission electron microscope (TEM) images were recorded on a TEM 2100F field emission transmission electron microscope. Fourier transform infrared (FTIR) spectroscopy was obtained on a Thermo Nicolet 5700. The concentration of Cr(VI)was analyzed on an induced coupled plasma atomic emission spectrometer (PE Optima 2100DV ICP-AES).

RESULTS AND DISCUSSION

After coating silica layer, sample 1 was tetragonal β-FeOOH (Fig. 1a, JCPDS File No. 34-1266). Obvious sign of the amorphous SiO_2 hump at Bragg angle of 20-35° was discerned. Samples 2 and 3 showed a similar XRD diffraction pattern to that of sample 1 (Fig. 1b and 1c). The relative intensity of amorphous SiO_2 hump increased with increasing the thickness of silica layer. After reaction with $NaBH_4$ at 50 °C for 0.5 h, it showed a similar XRD diffraction pattern to that of sample 2 (Fig. 1d). The hump at Bragg angle of 20-35° confirmed the presence of silica after reacted with $NaBH_4$. The existence of the silica layer could also be confirmed by FTIR spectra (Fig. 2). The characteristic peak at 1100, 958 and 802 cm^{-1} in FTIR spectrum was corresponding to the stretching vibrations of the terminal group in Si-O-Si and bond Si-O-R/Si-OH[10].

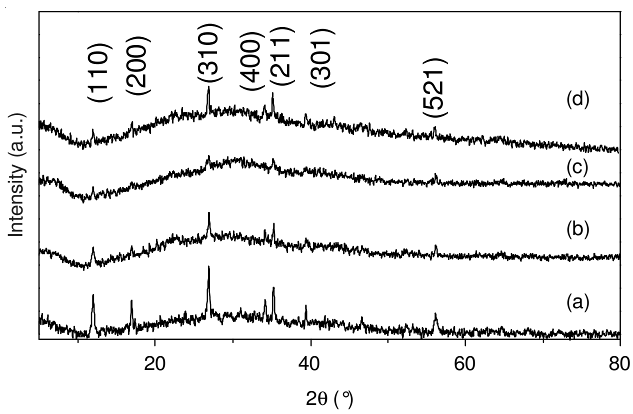

Fig. 1. XRD patterns of (a) sample 1, (b) sample 2, (c) sample 3, and (d) sample 2 after treatment with $NaBH_4$ for 0.5 h

β-FeOOH was nanorods with diameters of about 50 nm and lengths up to 300 nm (Fig. 3a). After coating the silica layer, sample 1 remained in rod-like shape with a similar size to that of β-FeOOH (Fig. 3b). TEM image confirmed the core-

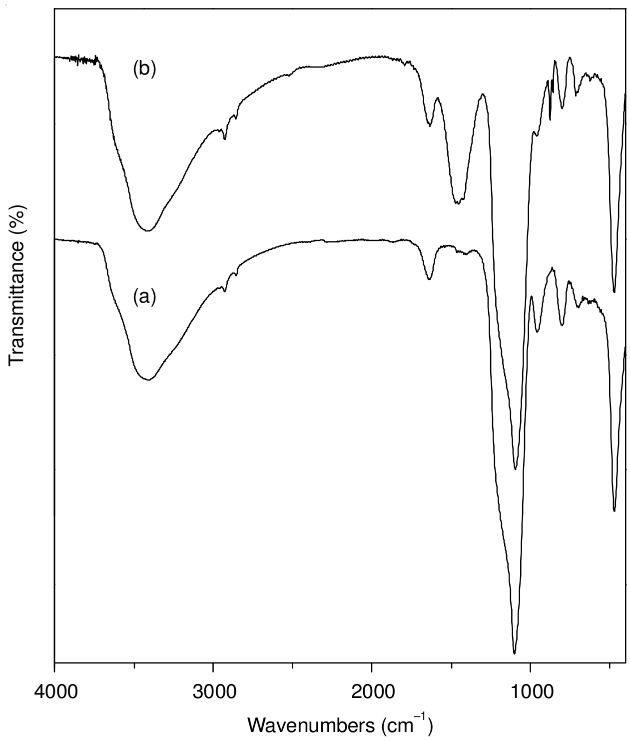

Fig. 2. FTIR spectra of (a) sample 2 and (b) sample 2 treated by $NaBH_4$ for 1 h

shell structure and the shell thickness was about 10 nm. By changing the mole ratio of ammonia to TEOS, sample 2 was core-shell structure with the shell thickness of 50 nm (Fig. 3c). After the second coating step, the thickness of silica layer increased to 100 nm (sample 3, Fig. 3d). By mixing with $NaBH_4$ at 50 °C for 1 h, sample 2 converted into yolk-shell structure with a core, a shell and the interstitial void between

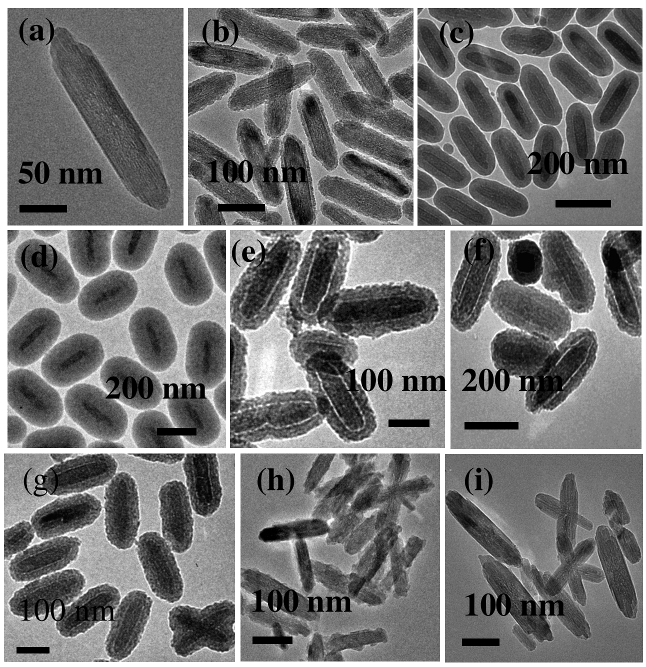

Fig. 3. TEM images of (a) β-FeOOH, (b) sample 1, (c) sample 2, and (d) sample 3, TEM images of samples in the presence of $NaBH_4$ after reacting with (e) sample 2 for 1 h, (f) sample 3 for 2 h, (g) sample 2 for 0.5 h, (h) sample 2 for 8 h, and (i) sample 1 for 1 h

the core and shell (Fig. 3e). The size of the interstitial void was about 10 nm. The silica layer was more porous compared with that of sample 2.

Fig. 4 illustrates the synthesis procedure for the yolk-shell structures. β-FeOOH/SiO_2 core-shell structures were prepared by Stober method. $NaBH_4$ reacted with water to form a strong base sodium metaborate ($NaBO_2$). Part of silica layer was dissolved in alkaline solution to form soluble silicates. Once the concentration of soluble silicates reached a critical value, silica can nucleate and grow into shells around the scaffold of un-dissolved silica layer. The new formed silica layer was more porous. It made the transformation of silicates from the interior side of silica layer to the outer side easier, gradually leading to the formation of the interior void between core and shell. The formation of interior void depends on the concentration of silicates in solution and the diffusion of silicates from interior side to outer side. So the thickness of the silica layer and reaction time influenced the formation of yolk-shell structures. Thinner silica layer (10 nm) could not offer enough Si source to form new porous layer on the surface of β-FeOOH. No silica layer was observed (Fig. 3i). When the thickness of silica layer was increased to 100 nm, longer reaction time was need to obtained yolk-shell structure (Fig. 3f). We also investigated the effect of reaction time. After reacting with $NaBH_4$ for shorter time (0.5 h), the sample remained the core-shell structure. No obvious interstitial void was observed (Fig. 3g). Prolong the reaction time to 8h, the core-shell structure was damaged and only a thin layer of silica was coated on the surface of β-FeOOH (Fig. 3h).

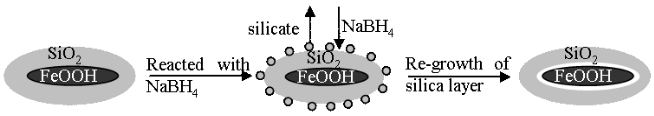

Fig. 4. Schematic illustration of the formation process of the yolk-shell structures

To evaluate the Cr(VI) adsorption capacity of yolk-shell structures, the adsorption isotherm was conducted (Fig. 5). The amount of Cr(VI) adsorbed at equilibrium (q_e) was increased with the increasing of C_e. Freundlich adsorption model ($\ln q_e = \ln C_e/n + \ln K_F$) was used to calculate the maximal adsorption capacity. The experimental data fitted well to the Freundlich adsorption model. The regression coefficient (R^2) was 0.993 (sample 2) and 0.964 (sample 2 treated with $NaBH_4$ for 1 h). This suggested that Cr(VI) adsorption behavior on β-FeOOH/silica yolk structure could be regarded as a multi-layer adsorption process. Compared with core-shell structures (sample 2), yolk-shell structures showed better adsorption ability. The maximal Cr(VI) removal capacity (q_m) for core-shell structures was 70.8258 mg/g while 221.7584 mg/g for yolk-shell structures within our experimental range. The maximal Cr(VI) removal capacity for yolk-shell structures was much higher than those reported for the Cr(VI) removal[11,12].

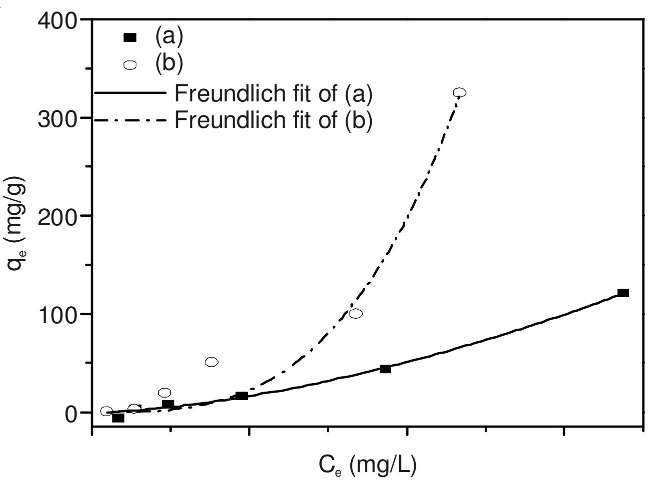

Fig. 5. Adsorption isotherms of Cr(VI) using (a) sample 2, (b) sample 2 after treatment with $NaBH_4$ for 1 h

Conclusion

β-FeOOH/silica yolk-shell structures were synthesized *via* a templating approach, based on controlling the reaction between $NaBH_4$ and β-FeOOH/silica core-shell structures. The concentration and diffusion process of soluble silicates influenced the formation of yolk-shell structures, which could be controlled by changing the thickness of silica layer and reaction time. With thinner silica layer, no yolk-shell structures were formed, while longer reaction time was necessary to form yolk-shell structures for thicker silica layer. Their adsorption activities were determined using aqueous solution of Cr(VI). The adsorption process fitted to Freundlich isotherm models. Due to the porous silica layer and the interior voids between β-FeOOH core and silica shell, β-FeOOH/silica yolk-shell structures exhibited a better Cr(VI) adsorption property.

ACKNOWLEDGEMENTS

Financial supports from Shandong Provincial Natural Science Foundation of China (No. ZR2010EM059), Shandong Education Department of International Cooperation Training Program (No. 2007:207091) and Development of Young Teachers Program of Shandong University of Technology (No. 4072:110019) are acknowledged.

REFERENCES

1. J.W. Liu, J. Cheng, R. Che, J. Xu, M. Liu and Z. Liu, *J. Phys. Chem. C*, **117**, 489 (2013).
2. Y. Zhu, Y. Fang and S. Kaskel, *J. Phys. Chem. C*, **114**, 16382 (2010).
3. Y. Chen, H. Chen, L. Guo, Q. He, F. Chen, J. Zhou, J. Feng and J. Shi, *ACS Nano*, **4**, 529 (2010).
4. J. Gao, G. Liang, B. Zhang, Y. Kuang, X. Zhang and B. Xu, *J. Am. Chem. Soc.*, **129**, 1428 (2007).
5. S. Linley, T. Leshuk and F.X. Gu, *ACS Appl. Mater. Interfaces*, **5**, 2540 (2013).
6. H. Li, Z. Bian, J. Zhu, D. Zhang, G. Li, Y. Huo, H. Li and Y. Lu, *J. Am. Chem. Soc.*, **129**, 8406 (2007).
7. X. Du and J. He, *ACS Appl. Mater. Interfaces*, **3**, 1269 (2011).
8. T. Zhang, Q. Zhang, J. Ge, J. Goebl, M. Sun, Y. Yan, Y. Liu, C. Chang, J. Guo and Y. Yin, *J. Phys. Chem. C*, **113**, 3168 (2009).
9. H.F. Shao, X.F. Qian, J. Yin and Z. Zhu, *J. Solid State Chem.*, **178**, 3130 (2005).
10. D. Li, W.Y. Teoh, R.C. Woodward, J.D. Cashion, C. Selomulya and R. Amal, *J. Phys. Chem. C*, **113**, 12040 (2009).
11. G. Cheng, J. Xiong, H. Yang, Z. Lu and R. Chen, *Mater. Lett.*, **77**, 25 (2012).
12. Z. Wu, S. Li, J. Wan and Y. Wang, *J. Mol. Liq.*, **170**, 25 (2012).